

THE EFFECT OF GRAVITY STRIPPING ON THE RESOLUTION OF DEEP CRUSTAL STRUCTURES IN THE EASTERN ALPS AND SURROUNDING REGIONS

Oliver SIMEONI & Ewald BRÜCKL[†]

KEYWORDS

Eastern Alps
density
gravity
Moho
crust

Vienna University of Technology, Institute of Geodesy and Geophysics, Gusshausstrasse 27-29, A-1040 Vienna, Austria;

[†] Corresponding author, ebrueckl@mail.tuwien.ac.at

ABSTRACT

Recent large-scale seismic experiments extended and refined existing crustal models of the Eastern Alps and their surrounding geologic provinces considerably. However, areas of low resolution and ambiguous interpretation still remain. The integration of gravity data has the potential to further constrain the seismic models of the crustal structure. In this study we concentrate on the gravity effect of the upper crust (max. depth 10 km). We apply gravity stripping of the upper crust and investigate its impact on resolution of deeper structures, especially the Moho-discontinuity. We derive one density model from a data set of sampled densities, and two others from relations between seismic velocity and density. Data from the exploration industry are implemented to determine the densities of Tertiary basins. We calculate the reduced gravity effects of these three models and their corresponding stripped Bouguer gravities. An analysis of the logarithmic power spectrum of the Bouguer anomaly reveals that wavenumbers greater than $k = 2\pi/92 \text{ km}^{-1}$ correspond to sources within the upper crust. We apply this wavenumber as a cut-off to separate the Bouguer anomaly, the reduced gravity effect, and the stripped Bouguer anomalies into high and low wavenumber parts. None of the three density models implemented in gravity stripping reduce the high wavenumber part of the Bouguer anomaly. However, we find that long wavelength density variations dominate the reduced gravity effect of the upper crust. Gravity stripping based on density models derived from seismic data significantly enhances the main structural features, which can be identified in the Moho depth map and are compatible with a lower crust – upper mantle density contrast of $\sim 300 \text{ kg/m}^3$.

Neue, großräumige seismische Experimente erweiterten und verbesserten bestehende Krustenmodelle der Ostalpen und deren umgebenden geologischen Provinzen erheblich. Allerdings verbleiben immer noch Gebiete mit niedriger Auflösung oder mehrdeutiger Interpretation. Die Integration von Schweredaten hat das Potential, die seismischen Modelle der Erdkruste weiter einzuschränken. In der vorliegenden Studie konzentrieren wir uns auf den Schwereeffekt der Oberkruste (max. Tiefe 10 km). Wir wenden Schwerereduktion für die Oberkruste an und untersuchen dessen Einfluss auf die Auflösung von tieferen Strukturen, insbesondere der Moho-Diskontinuität. Wir leiten ein Dichtemodell aus einem Datensatz von Dichteproben ab. Zwei weitere beruhen auf dem Zusammenhang zwischen seismischer Geschwindigkeit und Dichte. Für die Festlegung der Dichten Tertiärer Becken werden Daten der Explorationsindustrie verwendet. Wir berechnen die reduzierten Schwereeffekte dieser drei Modelle und die entsprechenden reduzierten Bougueranomalien. Eine Analyse des logarithmischen Leistungsspektrums der Bougueranomalie zeigt, dass Wellenzahlen über $k = 2\pi/92 \text{ km}^{-1}$ Quellen innerhalb der Oberkruste zugeordnet werden können. Wir trennen über diese Wellenzahl die Bouguer Anomalie, den reduzierten Schwereeffekt, und die reduzierten Bougueranomalien in hoch- und tieffrequente Anteile. Keines der drei Dichtemodelle führt zu einer Reduktion der hohen Wellenzahlanteile der reduzierten Bouguer Anomalien. Wir finden jedoch, dass langwellige Dichteveränderungen den reduzierten Schwereeffekt der Oberkruste dominieren. Schwerereduktion auf Basis der Dichtemodelle, die aus den seismischen Daten abgeleitet wurden, lässt die großräumige Struktur der Moho-Diskontinuität in den gravimetrischen Daten wesentlich besser erkennen und ist mit einem Dichtekontrast von $\sim 300 \text{ kg/m}^3$ zwischen Unterkruste und oberem Erdmantel kompatibel.

1. INTRODUCTION

The Eastern Alps and their surrounding geologic provinces pose a continuous attraction to geoscientists. Despite their large-scale geodynamic evolution being well understood in a general plate tectonic context (e.g., Stampfli and Kozur, 2006), specific geologic structures and tectonic processes are still a matter of debate. Examples for this situation are tomographic images of the upper mantle, which may be interpreted as a reversal of subduction between the European and Adriatic lithosphere (e.g., Kissling et al., 2006), or the many uncertainties in

the evolution of the Pannonian basin in between the Alpine, Carpathian, and Dinaric orogens (e.g., Wortel and Spakman, 2000; Horvath et al., 2006).

For about five decades, active source seismic experiments contributed significantly to our knowledge of the deep crustal structure, especially the depth of the Moho-discontinuity (e.g., Giese, 1976; Yan and Mechie, 1989; Brückl et al., 2007 and references therein). The recent large-scale seismic experiments TRANSALP (TRANSALP Working Group, 2002), CELE-

BRATION 2000 (Guterch et al., 2003), and ALP 2002 (Brückl et al., 2003) extended and refined existing crustal models considerably. However, areas of low resolution and ambiguous interpretation still remain.

Like seismic investigations, gravity studies have a long history within the scope of exploration of the deep crustal structure of the Eastern Alps (e.g., Meurers et al., 1987; Granser et al., 1989; Lillie et al., 1994; Ebbing, 2004; Ebbing et al., 2006). A pilot study on the integration of gravity data (Kraiger and Kühtreiber, 1992) and seismic models derived from the recent large-scale seismic experiments was carried out by Brückl et al. (2006). The new Bouguer anomaly map of Central Europe, including the Eastern Alps in the investigation area of ALP 2002, by Bielik et al. (2006) is our motivation to continue this study on the basis of the new gravity data.

The interpretation of gravity data without additional constraints is ambiguous. Gravity stripping with the implementation of additional geological or geophysical data, however, can tackle this problem. We apply this technique to the upper crust (max. depth 10 km) and investigate its impact on the resolution of deeper structures, especially the Moho-discontinuity.

2. STUDY AREA – GEOLOGY AND CRUSTAL STRUCTURE

The study area extends over longitudes of approximately 11°-20°E and latitudes 45°-51°N. The major geological units belong – from north to south – to the Bohemian Massif, the Flysch belt and the Outer Carpathians, the Eastern Alps and the Inner Carpathians, the Southern Alps, the Dinarides, and the Adriatic Foreland. Penninic windows were exhumed in the Eastern Alps (Engadin, Tauern and Rechnitz window). Large Tertiary sedimentary basins are the Molasse basin, the Styrian and Vienna basins, the Po plain, and the Pannonian basin with their different depositional centres. Fig. 1 shows these major geological units superimposed on a digital elevation model.

Crustal structures of high relevance for gravity studies are the Tertiary sedimentary basins, especially knowing the depth of their base. Fig. 2 shows this data in our area of interest. Another source which contributes to variations of the gravity field is the density contrast between lighter crustal rocks and the denser mantle at the Moho-discontinuity. Behm et al. (2007) generated a map of the Moho depth from data of the CELEBRATION 2000 and ALP 2002 seismic experiments. To the west, we also integrated the results of the TRANSALP transect (e.g. Lüschen et al., 2004; 2006). This map has been extended using data from Ziegler and Dèzes (2006) to supply Moho depths for the whole study area (Fig. 3).

3. BOUGUER ANOMALY

We used the Bouguer gravity data from Bielik et al. (2006), which covers most of our investigation area. Inside Austria, this data is identical to the Bouguer gravity map of Meurers and Ruess (2007). Areas which are not covered by the gravity data of Bielik et al. (2006) have been supplemented by the regional Bouguer gravity map of the West-East Europe Gravity

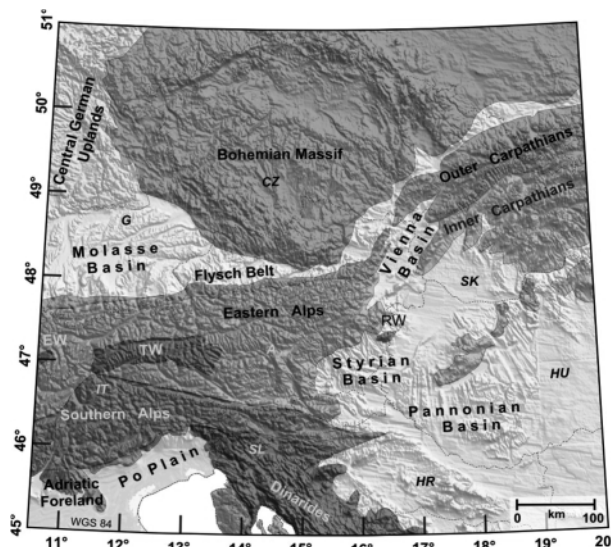


FIGURE 1: Investigation area: major geological units superimposed on DTM. The geological units were generalized after Schmid et al. (2004), Oberhauser (1980), and Franke and Żelaźniewicz (2000).

Project, WEEGP (<http://www.getech.com>). The original data have a grid spacing of 2x2 km (Bielik et al., 2006) and 9.2 x 9.2 km (WEEGP). We resampled the data to the grid spacing of the Moho map (20x20 km grid) after smoothing with a Hanning convolution matrix in order to homogenize the gravimetric and seismic data sets (Fig. 4). A first comparison between the Bouguer anomaly (BA) and the Moho depths (Fig. 3) shows a negative correlation, as expected from isostasy. The effect is very pronounced for the main body of the Eastern Alps, the Pannonian basin, and the Po plain. The negative correlation can be recognized, but is less prominent for the West Carpathians and the Dinarides.

The 2D power spectrum $E(k)$ of the BA is shown in Fig. 5. The wavenumber (k) is related to the wavelength (λ) in the horizontal X-Y plane by $k = 2\pi/\lambda$. Furthermore, were averaged

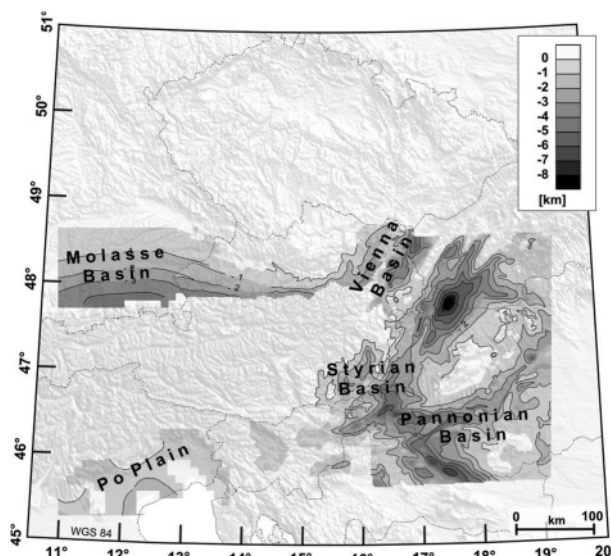


FIGURE 2: Investigation area: depth of Tertiary basins superimposed on DTM.

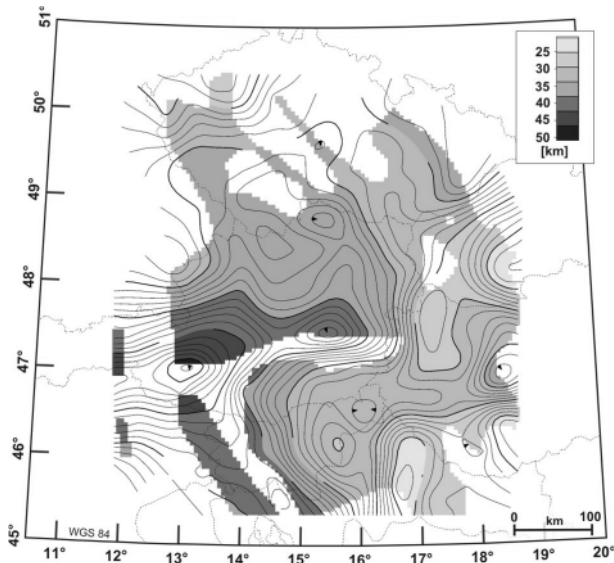


FIGURE 3: Moho depth map (Behm et al., 2007) and Moho depth at TRANSALP (Lüschen et al., 2004); colour code shows data, contour lines interpolate data areas. This compilation has a grid spacing in X and Y of 20 km. The data are smoothed by convolution with a Hanning 3x3 matrix.

the spectral amplitudes over wavenumber intervals of $k = 2\pi/620 \text{ km}^{-1}$ concerning smoothing.

If the potential field observed at a constant depth h exhibits a white power spectrum, then the power spectrum of the field observed at the surface ($h=0$) is proportional to $\exp(-2hk)$ and, therefore, the slope of $\ln(E)$ over k at the surface is $-2h$ (e.g., Cianciara and Marcak, 1976; Buttkus, 1991). We approximated the logarithmic power spectrum $\ln(E)$ by 2 straight lines with different slopes, which represent randomly distributed point sources at maximum depths of 40 km and 12 km. The value with the lowest wavenumber does not fit to the straight lines and indicates even deeper sources (Fig. 5).

Depth estimates on the basis of logarithmic power spectra represent the maximum depth in which randomly distributed

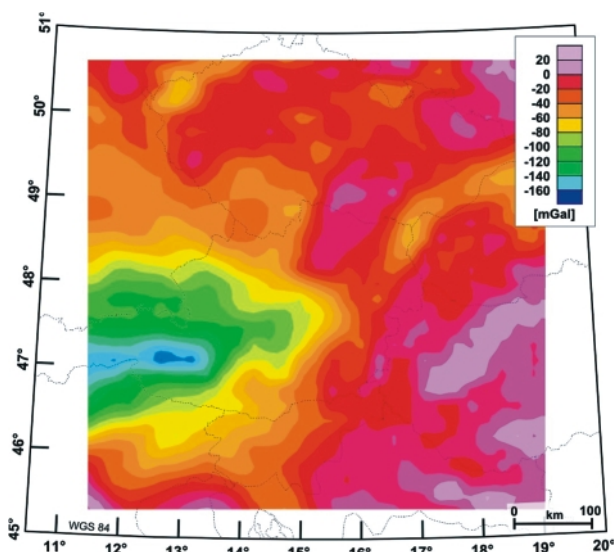


FIGURE 4: Bouguer anomaly (Bielik et al., 2006).

point sources could be located. Therefore, the depth estimates of $h = 40 \text{ km}$ correspond to Moho topography and long wavelength crustal density variations. The depth estimates of $h = 12 \text{ km}$ correspond to density anomalies in the upper crust, probably at less than 10 km depth. The power spectrum was decomposed into a long wavelength and a short wavelength component. When choosing the cut-off wavelength we used the intersection of the 2 straight lines in Fig. 5. The cut-off wavelength of the high pass is 92 km ($k = 0.0685 \text{ km}^{-1}$) and the slope of the filter is $-3.3\text{dB}/0.01k$. The filters are chosen so that the sum of high and low pass filtered field gives the same power spectrum as the non-filtered field. The corresponding low and high pass filtered Bouguer anomalies (BA_{lp} and BA_{hp}) are shown in Fig. 6a (BA_{lp}) and Fig. 6b (BA_{hp}). A comparison of BA (Fig. 4) with BA_{lp} and BA_{hp} suggests that BA is dominated by the low wavenumber structures ($\lambda > 92 \text{ km}$). At first glance, BA_{hp} may appear to be a random pattern. However, a closer inspection shows several features, which correlate well with surface geology. We marked two gravity lows and one gravity high in Fig. 6b; that is, the Tauern Window, the Vienna basin, and the Gurktal nappes. Other high-wavenumber anomalies, not identified in Fig. 6b are, for example, the Eger-Graben, the Bohemian Batholiths, the Mid-Hungarian Range, and Istria.

4. DENSITY DATA

In the following, we consider the different sources of information of upper crust density used for our study.

4.1 APPARENT DENSITY

Granser et al. (1989) used the high wavenumber component ($k < 2\pi/100 \text{ km}^{-1}$) of the Bouguer anomaly (BA) map by Senftl (1965) to calculate the apparent density. According to their analysis of the power spectrum, the maximum depth of the corresponding sources is 9 km. An algorithm based on convolution of the high wavenumber component of the BA was applied to calculate the apparent density. Therefore, the gravity effect of a crust with apparent density perfectly matches the high pass filtered BA. The investigation area of Granser et al. (1989) is not identical with our region of interest. Fig. 7 shows the apparent density data available in our area. When comparing the apparent density in Fig. 7 with BA_{hp} in Fig. 6b, the same structures can be identified. Stripping the gravity effect of the upper crust from the BA with a density model based on the apparent density is identical to low pass filtering. Differences to our data arise only because Granser et al. (1989) had the older data set of Senftl (1965).

4.2 DENSITIES OF TERTIARY BASINS

Hydrocarbon exploration in Tertiary basins yielded a wealth of density information about these strata. Here we present existing relations derived by regression for the different basins. Information on the density of the Tertiary basins was considered to be the most accurate. Therefore, it will be used in all our density models. In all relations, density (ρ) will be in

kg/m³ and depth (z) from surface in km.

4.2.1 MOLASSE BASIN

Fischer (2004) derived the following depth-density relationship for the Molasse basin from seismic check shot data and their conversion to densities. The check shot data were supplied by courtesy of RAG (Rohöl-Aufsuchungs Gesellschaft m. b. H., Wien):

$$\rho = 2710 - 400 \exp(-0.75 \cdot z).$$

4.2.2 VIENNA BASIN

Granser (1987) used the following depth-density function gravity modelling of the Vienna basin:

$$\rho = 2650 - 450 \cdot \exp(-0.65 \cdot z).$$

4.2.3 STYRIAN BASIN

For the gravity modelling of the Styrian basin, Sachsenhofer et al. (1996) introduced the depth-density function:

$$\rho = 2710 - 510 \cdot \exp(-0.65 \cdot z).$$

4.2.4 PANNONIAN BASIN

For the gravity modelling of the Pannonian basin, we transformed the discrete depth-density data supplied by Makarenko et al. (2002) into the following third-order polynomial:

$$\rho = 2140 + 220 \cdot z - 37.4 \cdot z^2 + 2.58 \cdot z^3.$$

We use the same depth-density function for the Po plain as for the Molasse basin.

4.3 DENSITIES FROM SAMPLES

A surface density model has been derived in Austria and the surrounding areas mainly by density measurements of rock samples collected at the surface or near-surface locations (e.g., Meurers et al., 1990; Granser et al., 1983; Walach, 1987). The latest version of this model, which also considers the sea, has

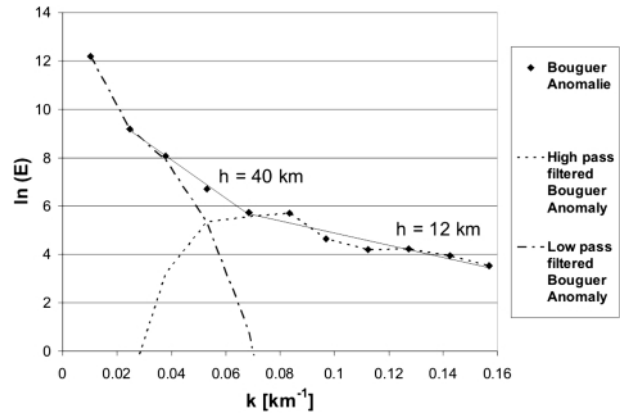


FIGURE 5: Wave number analysis of Bouguer anomaly; (a) logarithmic power spectrum and maximum depth of sources derived from slope of regression lines.

been provided by B. Meurers (pers. communication). Fig. 8a shows this density model for our study area. A comparison of the density map with the geological map shows clearly that density values were treated separately for the different geological units.

In our investigation, we test if these surface densities are representative for the whole upper crust and useful for gravity stripping. We are aware that this was not the original purpose of the density model. However, Granser et al. (1989) did find some correlations between apparent density of the upper crust and the surface density k model. It would not make sense to extrapolate surface densities of Tertiary basins and similar sediments through the upper crust. Only Mesozoic rocks or the crystalline basement exposed at the surface could yield an acceptable estimate of the density of the basement. We considered only surface densities >2450 kg/m³ for a density estimate of the crustal basement, which was roughly identical to the exclusion of the Tertiary basins, the Quaternary valley

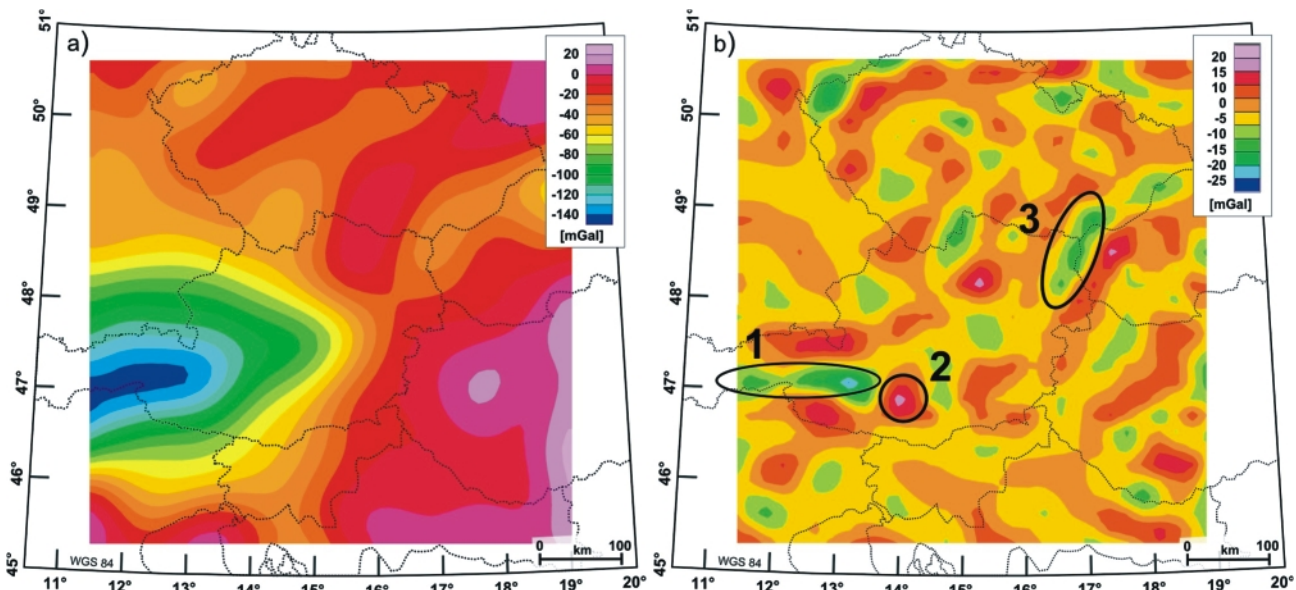


FIGURE 6: Bouguer anomaly; (a) low-wavenumber component; (b) high-wavenumber component; the two ellipses and the circle mark geologic units representing density contrasts (1 – Tauern window, 2 – Gurktal nappe, 3 – Vienna basin).

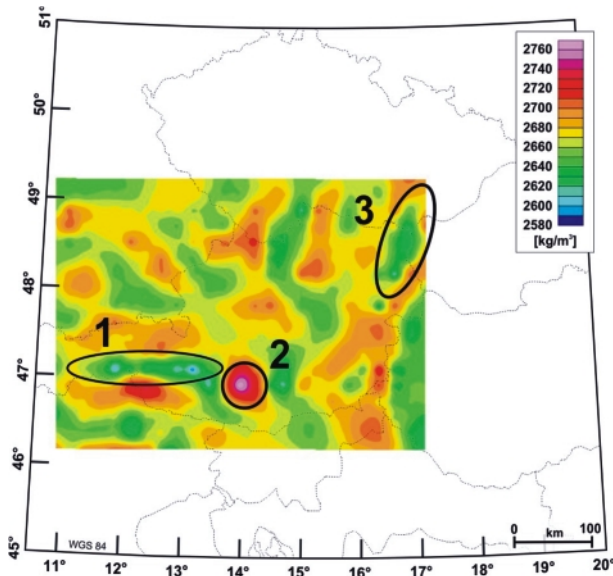


FIGURE 7: Apparent density (Granser, 1989); the two ellipses and the circle mark the same geologic units as in Fig. 6b.

fills and the Flysch belt. Fig. 8b shows this density data extrapolated to the whole investigation area.

5. DERIVATION OF DENSITY FROM SEISMIC DATA

Relations between seismic velocity (mainly P-wave velocity, V_p) and rock density (d) have been established from global data, as well as from data collected during hydrocarbon exploration and similar activities. The CELEBRATION 2000 and ALP 2002 seismic experiments (Guterch et al., 2003; Brückl et al., 2003) brought a wealth of new data on seismic velocities, which we intend to use for the determination of a density mo-

del of the upper crust. Fig. 9 shows depth slices at 0 km, 5 km, and 10 km through the 3D P-wave velocity model of Behm et al. (2007). Near surface, at the depth $z = 0$ km, the low velocities of the Tertiary basins are the dominating structures. At $z = 5$ km and even at $z = 10$ km, we still see relatively low velocities below the basins. Relatively high velocities form a belt north of the Tauern window. An exceptional velocity high correlates roughly with the Adriatic foreland. We apply the following V_p -density relations to convert the V_p -model to a density model. In the formula given below, V_p is given in km/s and the density (ρ) again in kg/m^3 .

5.1 GARDNER

Gardner's rule (Gardner et al., 1974) has been derived for sedimentary rocks (Gulf of Mexico).

$$\rho = 1740 \cdot V_p^{0.25}$$

5.2 NAFE-DRAKE

In this paper, we use the polynomial approximation of the Nafe-Drake V_p -density relation given by Brocher (2005). Like the Gardner relation, this is based on data from the Gulf of Mexico.

$$\rho = 1661 \cdot V_p - 472 \cdot V_p^2 + 67.1 \cdot V_p^3 - 4.3 \cdot V_p^4 + 0.106 \cdot V_p^5$$

5.3 CHRISTENSEN-MOONEY

We use the following V_p -density relation derived by Christensen and Mooney (1995) for the upper crust:

$$\rho = 983.3 + 289.1 \cdot V_p$$

5.4 SOBOLLEV-BABEYKO

Sobolev and Babeyko (1994) reduced the in-situ velocity V_p

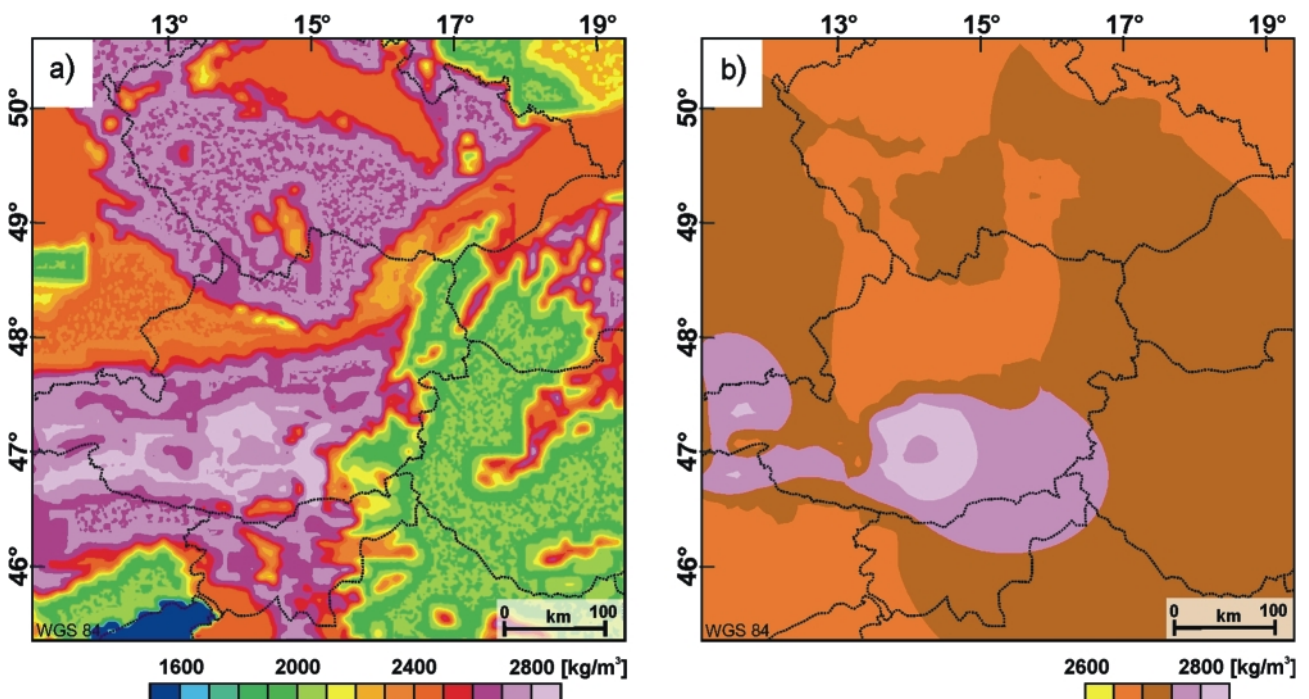


FIGURE 8: Densities from samples with a grid interval in X and Y of 6.4 km.; (a) whole data; (b) inter- and extrapolated data representing basement below Tertiary basins and Flysch belt.

to the corresponding value Vp_0 at the surface, considering a temperature (T) dependence of $-4.5 \cdot 10^{-4} \text{ km s}^{-1}/^\circ\text{C}$ and a pressure dependence of $0.12 \text{ km s}^{-1}/\text{GPa}$. We assume a temperature gradient of $25 \text{ }^\circ\text{C}/\text{km}$ and a pressure gradient of $0.0275 \text{ GPa}/\text{km}$. Thereafter, Vp_0 is converted to density at surface conditions (ρ_0) by:

$$\rho_0 = 446 \cdot Vp_0 - 74.$$

This relation is valid for $6.05 \text{ km s}^{-1} \leq Vp \leq 6.95 \text{ km s}^{-1}$. However, as no relation is given for Vp below 6.05 km s^{-1} , we also apply it to the lower Vp values. The final step is the transformation of d_0 to the in-situ density (ρ), assuming a temperature dependence of $-0.09 \text{ kg m}^{-3}/^\circ\text{C}$, and pressure dependence of $50 \text{ kg m}^{-3}/\text{GPa}$.

5.5 CORRELATION OF VP WITH DENSITY FROM SAMPLES

We investigate the correlation of Vp with the density from samples in the area outside the Tertiary basins. The question is, if we should take Vp from the surface ($z = 0 \text{ km}$), or from some deeper level. Fig. 10 shows the average Vp velocity over depth calculated from all values outside the Tertiary basins. From surface to a depth of about $z = 4.5 \text{ km}$, we observe a significant, but continuously decreasing gradient with depth. We interpret this velocity gradient as the closure of voids (open cracks and similar) due to increasing pressure and not as an effect of changing lithology. In case the density from samples represents the rock mass, including the effect of voids, the correlation with Vp at $z = 0 \text{ km}$ (open cracks) would be appropriate. In case the density of samples represents the rock material without the effect of open cracks etc., the correlation with Vp at $z = 4.5 \text{ km}$ (closed cracks) would be more adequate.

Fig. 11 shows correlations of density from samples with Vp (a) at $z = 0 \text{ km}$, and (b) at $z = 4.5 \text{ km}$. The centre of mean density data and the Vp -density relations of Nafe-Drake, Gardner, Christensen - Mooney, and Sobolev - Babeyko are also plotted. Both correlations have approximately the same slope. The linear correlation of density from samples with Vp at $z = 0 \text{ km}$ (Fig. 11a) yields systematically higher densities

Density model	Reduced gravity effect of upper crust (0-10 km depth)	Stripped Bouguer Anomaly
S	RG_S	BA_S
C	RG_C	BA_C
L	RG_L	BA_L

TABLE 1: Investigation area: major geological units superimposed on DTM. The geological units were generalized after Schmid et al. (2004), Oberhauser (1980), and Franke and Żelaźniewicz (2000).

than the other relations. The coefficient of determination is $r^2=0.034$. The linear correlation with Vp at $z = 4.5 \text{ km}$ (Fig. 11b) fits closely to the Gardner relation. The coefficient of determination is $r^2=0.047$. Nafe-Drake and Christensen - Mooney are also close to the data centre of the densities from samples, but have a steeper slope. The Sobolev - Babeyko relation yields systematically lower densities for Vp taken from $z = 0 \text{ km}$, as well as from $z = 4.5 \text{ km}$. Because of the better fit of density from samples with Vp at $z = 4.5 \text{ km}$ with the other relations, we assume that the density from samples represents the density of the rock material and not the rock mass.

The new relation between density from samples and Vp at $z = 4.5 \text{ km}$ (Fig. 11b) is:

$$\rho = 2072 + 108.2 \cdot Vp.$$

The new relation will be referred to as the "local relation" from here on. It is very similar to the Gardner relation in the Vp -range of $5.6 - 6.4 \text{ km/s}$.

6. DENSITY MODELS AND GRAVITY STRIPPING

We construct three density models of the upper crust. These models have the density of the Tertiary basins in common, which is given by the depth-density relations mentioned in 4.2. Inner-Alpine basins or deep valleys are not considered. The three models are identified by the extensions S, C, and L, and differ by the method we applied to determine the densities below the Tertiary basins:

- S – density from samples with interpolated values in the

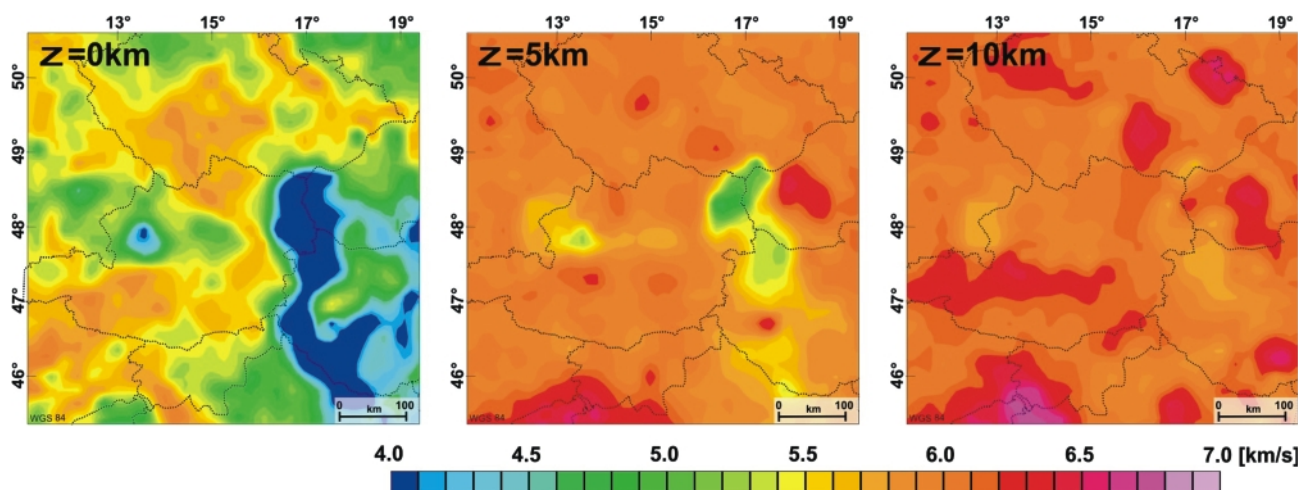


FIGURE 9: Depth slices at ($z = 0 \text{ km}$, 5 km , and 10 km) through the 3D Vp -velocity model of the upper crust (Behm et al., 2007).

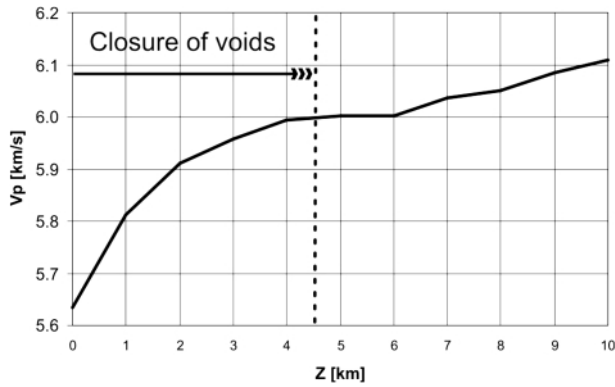


FIGURE 10: Average V_p -depth relation of upper crust, indicating the closing of voids between the surface and $z = 4.5$ km (for explanation see text).

areas of the Tertiary basins according to Fig. 8b,

- C – V_p of the 3D seismic model converted to density by the V_p -density relation of Christensen - Mooney,
- L – V_p of the 3D seismic model converted to density by the local V_p -density relation.

In order to reduce boundary effects in our calculations of the gravity effects, we extended the density model by 200 km in all directions. For this extension, we took a constant density of $\rho = 2670$ kg/m³ for the basement. The depth-density relations given in chapter 4.2 were also applied to the Tertiary basins in the extended area. The Adriatic Sea was approximated by a constant depth of 100 metres and a density of $d = 1000$ kg/m³. The gravity data over the Adriatic Sea are Free Air anomalies.

We calculated the gravity effects of the three density models by the method of Nagy (1966) for rectangular prisms with length x width x height = 20 km x 20 km x 1 km. As a reference we chose a homogeneous crust with a constant density of 2670 kg/m³ and 10 km thickness. These gravity effects of the different density models were reduced by the gravity effect of a homogeneous upper crust. Thereafter, gravity stripping of the upper crust was applied to the Bouguer anomaly (BA) by subtracting the different reduced gravity effects. The abbreviations subsequently used are compiled in Table 1. We also

applied high-pass (hp) and low-pass (lp) filtering to different reduced gravity effects and stripped Bouguer anomalies as described before. We identify the high-pass and low-pass components of this data by the extensions $_{hp}$ and $_{lp}$.

The reduced gravity effects for the different density models are shown in Fig. 12 together with their high and low pass filtered versions. The corresponding maps of the stripped Bouguer anomalies are shown in Fig. 13. Wavenumber filtering produces edge effects, which have no relation to geological structures. Therefore, we concentrate our further analysis of the filtered data on a restricted area and neglect an 80 km wide outer rim of the total area.

A first inspection of Figs. 12 and 13 reveals that the low wavenumber component dominates the reduced gravity effects (RG_{*}) and the stripped Bouguer anomalies (BA_{*}). Further, the gravity range of RG_C is significantly higher than the gravity ranges of RG_L and RG_S . Apparently, gravity stripping by RG_C modifies the BA the most. This also becomes evident if we consider the relations between the gravity effect caused by the varying Moho depth and BA_{lp} , $BA_{S_{lp}}$, $BA_{C_{lp}}$ and $BA_{L_{lp}}$ (Fig. 14). We calculated this gravity effect with a constant density contrast of 300 kg/m³ between lower crust and upper mantle, relative to an average Moho depth of 33 km by the method of Nagy (1966). The slopes of the cross plots of BA_{lp} , $BA_{S_{lp}}$, $BA_{C_{lp}}$, and $BA_{L_{lp}}$ over the gravity effect of the varying Moho depth deviates from 1:1, indicating that the density contrast was not chosen properly. In order to establish a 1:1 relation we multiplied 300 kg/m³ with the slope of the trend lines and obtained the density contrasts between the upper mantle and lower crust for each $BA_{*_{lp}}$ and BA_{lp} (Table 2). Gravity stripping by the models based on seismic data ($BA_{C_{lp}}$ and $BA_{L_{lp}}$) lead to density contrasts near 300 kg/m³, $BA_{S_{lp}}$ and BA_{lp} suggest significantly lower values.

Next, we consider correlations of the high wavenumber components of the reduced gravity effects ($RG_{*_{hp}}$) with the high wavenumber component of the Bouguer anomaly (BA_{hp}). BA_{hp} must have its sources within the upper crust. Therefore $RG_{*_{hp}}$ should approximate BA_{hp} . All reduced gravity

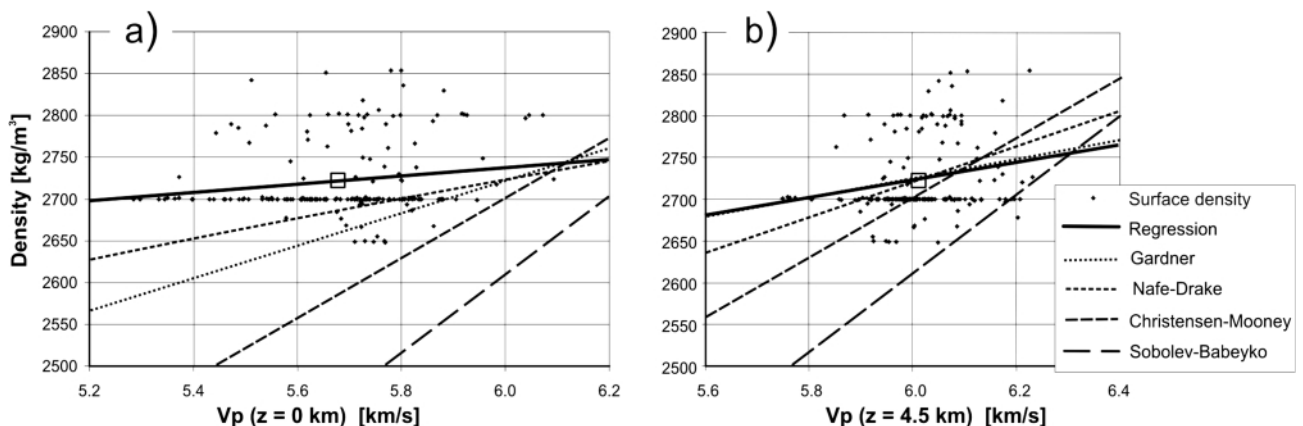


FIGURE 11: Correlations of density from samples with V_p (a) at $z = 0$ km, and (b) at $z = 4.5$ km; large square represents centre of the density data; lines show the V_p -density relations of Nafe-Drake, Gardner, Christensen - Mooney, and Sobolev – Babeyko.

effects indicate low correlations. The variances of BA_hp, BA_S_hp, BA_C_hp, BA_L_hp are compiled in Table 3. The variances of BA_S_hp, BA_C_hp, and BA_L_hp are in a similar range, but about 50% higher than the variance of BA_hp. Therefore, we state that none of the three density models approximated the real high wavenumber density anomalies in the upper crust to a sufficient degree of accuracy. Recently Meurers and Ruess (2009) presented a new Bouguer gravity map of Austria. They found that the implementation of surface density data (Granser et al., 1983) into the mass reduction may have an effect of up to 20 mGal. This aspect should be considered in future studies.

BA_lp	BA_S_lp	BA_C_lp	BA_L_lp
197 kg/m ³	245 kg/m ³	322 kg/m ³	279 kg/m ³

TABLE 2: Density contrast between lower crust and upper mantle estimated from the relation between Moho depth and Bouguer anomaly (BA) and stripped Bouguer anomalies (BA_*).

The performance of gravity stripping by the S, C, and L density models is poor in the high-wavenumber component of the power spectrum. However, as the high-wavenumber component is small compared to the low-wavenumber component, this is not a severe disadvantage. The low-wavenumber com-

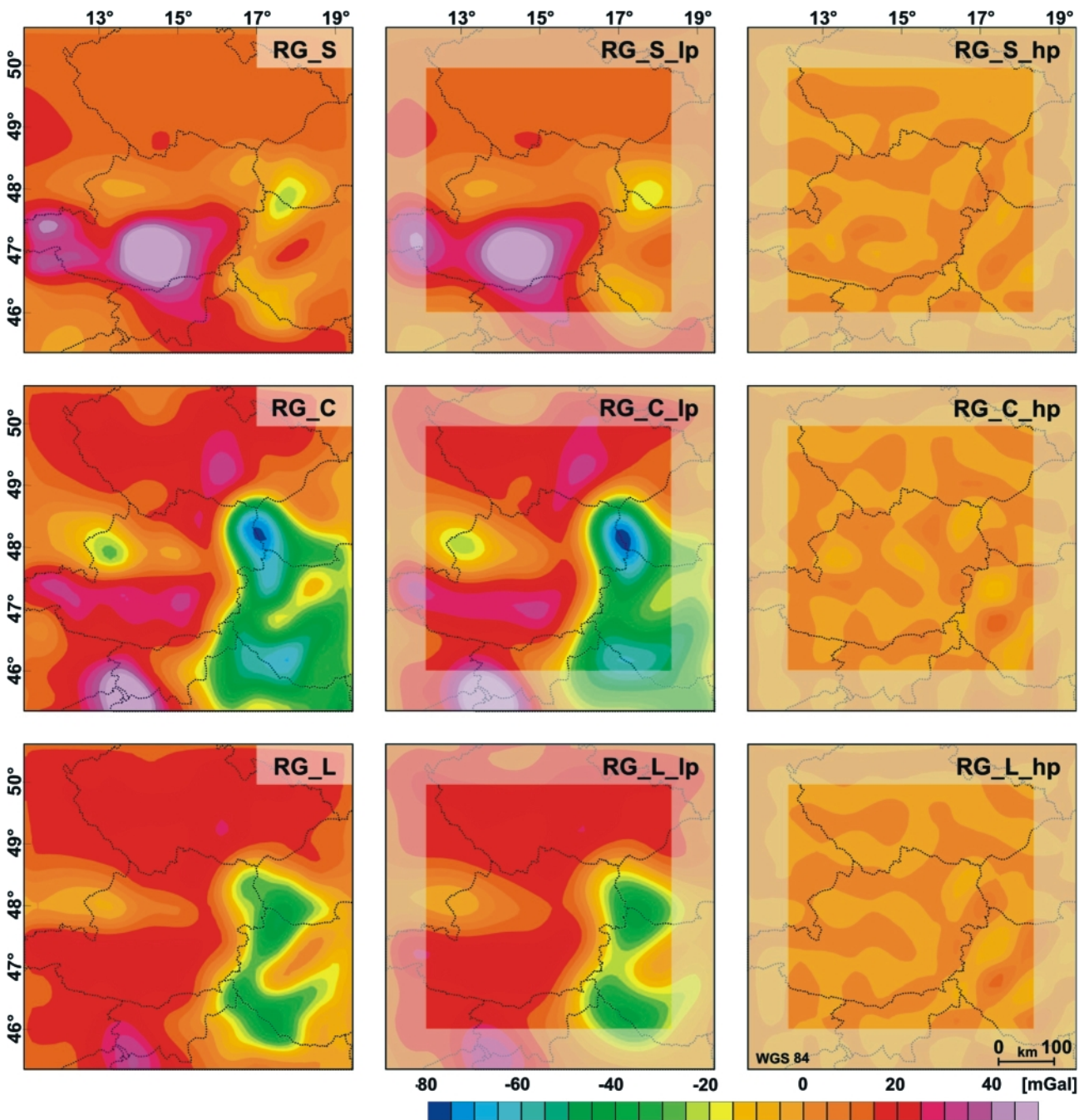


FIGURE 1 2: Reduced gravity effects of upper crust; column 1: RS_S in row 1, RS_C in row 2, RS_L in row 3; column 2: low pass components; column 3: high pass components; shading of the outer rim of filtered data indicates possible edge effects.

BA_hp	BA_S_hp	BA_C_hp	BA_L_hp
33 mGal ²	49 mGal ²	54 mGal ²	48 mGal ²

TABLE 3: Variances of the high wave number components of the Bouguer anomaly (BA_hp) and the stripped Bouguer anomalies (BA_S_hp, BA_C_hp, BA_L_hp).

ponent is significantly enhanced by gravity stripping with the C and L density model. A criterion to opt for the C model could be that BA_C best matches the Moho topography, especially at the bifurcation between the Eastern Alps and the Dinarides, and the transition from the thicker Alpine to the thinner Pan-

nonian crust (Fig. 13). We assembled diagrams of the BA, the Moho depth, and BA_C in Fig. 15 and chose an appropriate colour code to emphasize this effect of gravity stripping.

7. CONCLUSIONS

During the last decade, large-scale seismic experiments markedly increased our knowledge about the crustal structure of the Eastern Alps. The integration of new Bouguer gravity data (Bielik et al., 2006; Meurers and Ruess, 2007) has the potential to further refine and extend the image of these deep structures. The Bouguer anomaly clearly reflects the large lithospheric structures, especially the Moho depth. However, den-

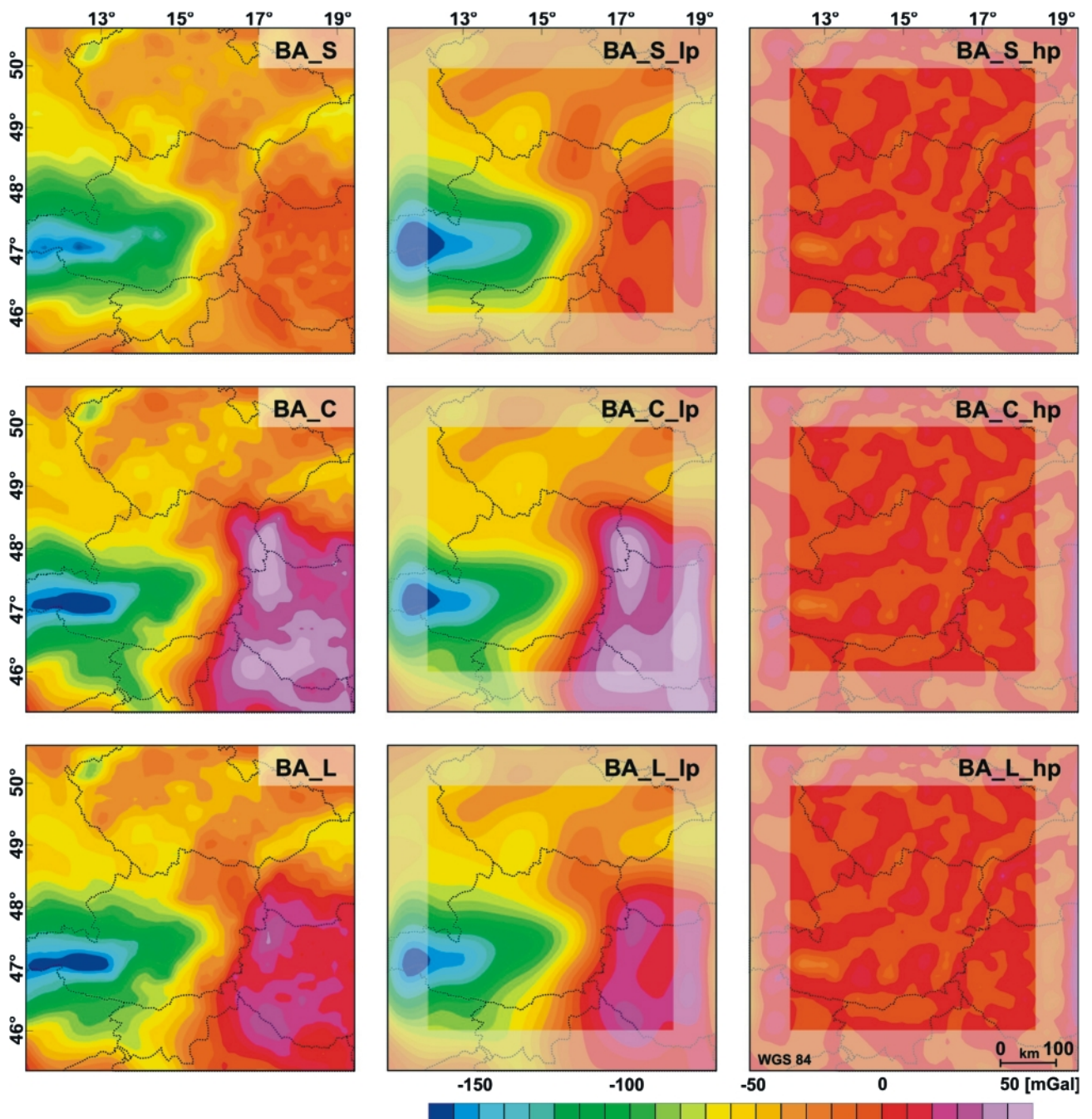


FIGURE 13: Stripped Bouguer anomalies; column 1: BA_S in row 1, BA_C in row 2, BA_L in row 3; column 2: low pass components; column 3: high pass components; shading of the outer rim of filtered data indicates possible edge effects.

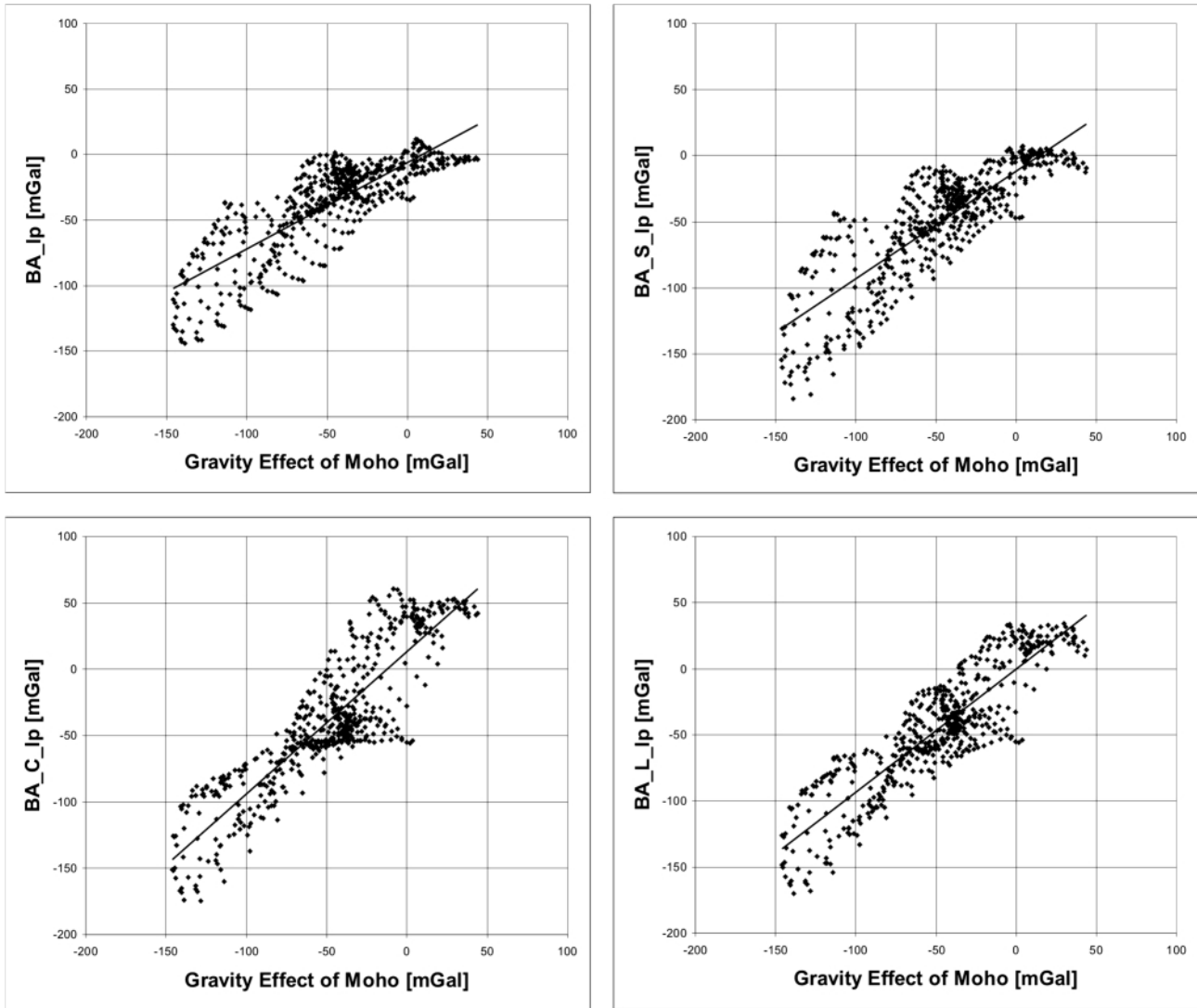


FIGURE 14: Cross plots of (a) low pass filtered Bouguer anomaly (BA_{lp}) and (b – d) low pass filtered stripped Bouguer anomalies (BA_{S_lp}, BA_{C_lp}, BA_{L_lp}) over the gravity effect related to the varying Moho depth, assuming a density contrast of 300 kg/m³ between lower crust and upper mantle.

ity anomalies in the upper crust severely distort the Bouguer anomaly and make the interpretation ambiguous. Gravity stripping provide an appropriate technique to reduce this ambiguity and to enhance the benefit of integrating gravity data into the

structural interpretation.

Spectral analysis of the Bouguer gravity data showed that the wavelength $\lambda < 92$ km is due to density anomalies located in the upper crust. We used this wavelength to separate gravity

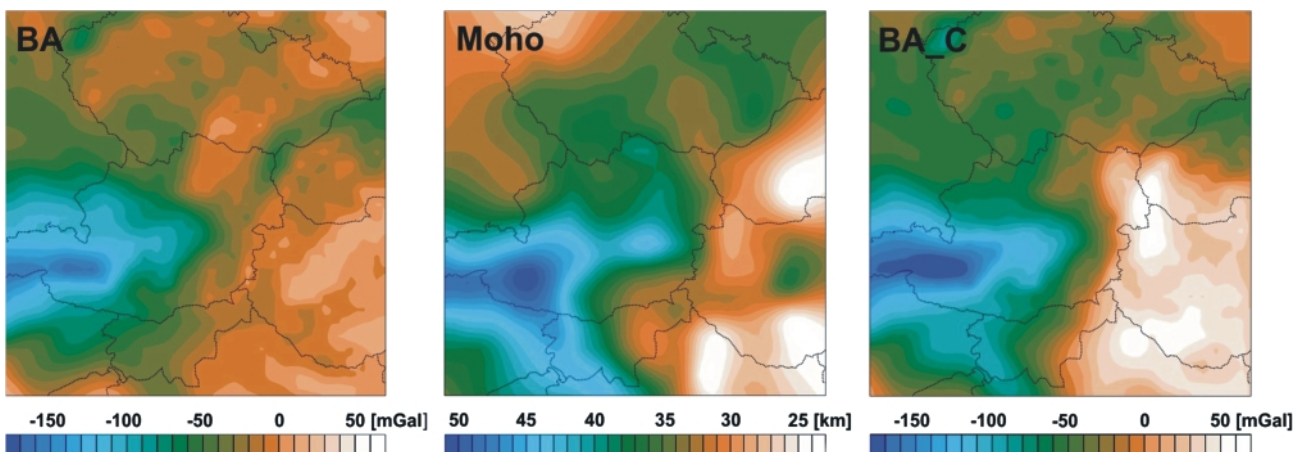


FIGURE 15: Comparison of Bouguer anomaly BA (left), Moho depth (middle), and stripped Bouguer anomaly BA_C (right).

signals into their high- and low-wavenumber components. The high-wavenumber sources have a maximum depth of 12 km and are therefore most probably located in the upper crust (< 10 km), while the low-wavenumber component is dominated by the deep structures (e.g. Moho), but can also have wide spreading sources in the upper crust. Optimal gravity stripping of the upper crust should result in a suppression of the Bouguer anomaly's high-wavenumber component and a compensation for the low-wavenumber component in the upper crust.

We generated three density models; one based on density data from samples (S), two others derived from Vp-density relations (C and L). The relation between Vp in the upper crust and density from samples indicates that these densities represent the rock material and not the in-situ rock mass including voids. The densities of Tertiary basins were taken from depth-density relations established in the course of hydrocarbon exploration. The high-wavenumber components of the reduced gravity effects of all density models show low correlations with the high-wavenumber component of the Bouguer anomaly, and gravity stripping increases high-wavenumber noise. The low-wavenumber components dominate the reduced gravity effects and the stripped Bouguer anomalies. A comparison of the Bouguer anomaly (BA) and its stripped versions (BA_S, BA_C, BA_L) with the Moho depth map shows that stripping based on density models derived from seismic data (C and L) significantly enhances the main deep structures perceived in the gravity data. Furthermore, these stripped Bouguer anomalies (BA_C and BA_L) correlate well with the gravity effect related to the varying depth of the Moho and are compatible with a density contrast between lower crust and upper mantle of $\sim 300 \text{ kg/m}^3$, a widely accepted value.

ACKNOWLEDGEMENTS

The authors thank J. Ebbing and B. Meurers for their careful and constructive reviews, J. Brückl for the preparation of the figures, and K. Alten for editing the text.

REFERENCES

- Behm, M., Brückl, E., Chwatal, W. and Thybo, H., 2007. Application of stacking and inversion techniques to 3D wide-angle reflection and refraction seismic data of the Eastern Alps. *Geophysical Journal International*, *Geophys. J. Int.*, Volume 170, Issue 1, doi: 10.1111/j.1365-246X.2007.03393.x, 275-298.
- Bielik, M., Kloska, K., Meurers, B., Svancara, J., Wybraniec, S., Fancsik, T., Grad, M., Grand, T., Guterich, A., Katona, M., Krolkowski, C., Mikuska, J., Pasteka, R., Petecki, Z., Polechonska, O., Ruess, D., Szalajova, V., Sefara, J., Vozar, J., 2006. Gravity anomaly map of the CELEBRATION 2000 region. *Geologica Carpathica*, June 2006, 57, 3, 145-156.
- Brocher, M., 2005. Empirical Relations between Elastic Wave-speeds and Density in the Earth's Crust. *Bulletin of the Seismological Society of America*, Vol. 95, No. 6, December 2005, doi: 10.1785/0120050077, 2081-2092.
- Brückl, E., Bodoky, T., Hegedüs, E., Hrubcova, P., Gosar, A., Grad, M., Guterich, A., Hajnal, Z., Keller, G.R., Špicak, A., Sumanovac, F., Thybo, H., Weber, F. and ALP2002 WORKING GROUP, 2003. ALP2002 Seismic Experiment. *Studia geophysica geodaetica*, Academy of Sciences of the Czech Republic, Volume 47. ISSN 0039-3169, 671-679. 2003.
- Brückl, E., Mitterbauer, U., Behm, M. and Working Groups Celebration 2000 & ALP2002, 2006. Studies on Crustal Structure and Gravity in the Eastern Alps. In: F. Sanso and A.J. Gil (eds), *Geodetic Deformation Monitoring: From Geophysical to Engineering Roles*. IAG Symposium 131, Springer, pp. 181-192.
- Brückl, E., Bleibinhaus, F., Gosar, A., Grad, M., Guterich, A., Hrubcova, P., Keller, R., Majdanski, M., Sumanovac, F., Tiira, T., Yliniemi, J., Hegedüs, E., Thybo, H., 2007. Crustal structure due to collisional and escape tectonics in the Eastern Alps region based on profiles Alp01 and Alp02 from the ALP 2002 seismic experiment. *J. Geophys. Res.*, 112, B06308, doi:10.1029/2006JB004687.
- Buttkus, B., 1991. *Spektralanalyse und Filtertheorie in der angewandten Geophysik*. Springer Verlag, Berlin-Heidelberg, 650 pp.
- Christensen, N.I. and Mooney, W.D., 1995. Seismic velocity structure and composition of the continental crust: a global view. *J. Geophys. Res.* 100, 9761-9788.
- Cianciara, B. and Marcak, H., 1976. Interpretation of gravity anomalies by means of local power spectra. *Geophysical Prospecting*, 24, 273-286.
- Ebbing, J., 2004. The crustal structure of the Eastern Alps from a combination of 3D gravity modelling and isostatic investigations. *Tectonophysics*, 380(1-2), 80-104.
- Ebbing, J., Braitenberg, C. and Götze, H.J., 2006. The lithospheric density structure of the Eastern Alps. *Tectonophysics*, 414, 145-155.
- Fischer, N., 2004. *Die Modellierung der Sedimentbecken im Rahmen von ALP 2002*, Diploma Thesis, Institute of Geodesy and Geophysics, University of Technology Vienna, Austria.
- Franke, W. and Żelaźniewicz, A., 2000. The eastern termination of the Variscides: terrane correlation and kinematic evolution. In: W. Franke, W. Haak, O. Oncken, and D. Tanner (eds.), *Orogenic processes: quantification and modelling in the Variscan Belt*, Geological Society, London, Special Publications, 179, 63-85.
- Gardner, G.H.F., Gardner, L.W. and Gregory, A.R., 1974. Formation velocity and density – the diagnostic basics for stratigraphic traps. *Geophysics* 39, 770-780.

- Giese, P., 1976. Results of the Generalized Interpretation of the Deep-Seismic Sounding Data, in *Explosion Seismology in Central Europe - Data and Results*, edited by P. Giese, C. Prodehl, and A. Stein, *Crustal and Upper Mantle Structure in Europe*, No. 1, 201-214, Springer Verlag Berlin Heidelberg New York, 1976.
- Granser, H., Hösch, K., Steinhauser, P. and Zych, D., 1983. Über das Dichtemodell in Österreich. In: *Geod. Arb. Österreichs Int. Erdmessung*, III, 159-182.
- Granser, H., 1987. Three-dimensional interpretation of gravity data from sedimentary basins using an exponential density-depth function. *Geophysical Prospecting* 35, p. 1030-1041.
- Granser, H., Meurers, B. and Steinhauser, P., 1989. Apparent density mapping and 3D gravity inversion in the Eastern Alps. *Geoph. Prospecting*, 37, p. 279-292.
- Guterich, A., Grad, M., Keller, G.R., Posgay, K., Vozar, J., Špicak, A., Brückl, E., Hajnal, Z., Thybo, H., Selvi, O. and CELEBRATION 2000 experimental team, 2003. CELEBRATION 2000 Seismic Experiment. *Studia geophysica geodaetica*, Academy of Sciences of the Czech Republic, Volume 47. ISSN 0039-3169, 659-669. 2003.
- Horváth, F., Bada, G., Szafián, P., Tari, G., Ádám, A. and Cloething, S., 2006. Formation and deformation of the Pannonian basin: constraints from observational data. In: Gee, D.G. & Stephenson, R.A. (eds.), *European Lithosphere Dynamics*. Geological Society London Memoir, 32, London, pp. 191-206.
- Kissling, E., Schmid, S.M., Lippitsch, R., Ansoerge, J. and Fügenschuh, B., 2006. Lithosphere structure and tectonic evolution of the Alpine arc: new evidence from high-resolution teleseismic tomography. In: Gee, D.G. & Stephenson, R.A. (eds.), *European Lithosphere Dynamics*. Geological Society London Memoir, 32, London, pp. 129-145.
- Kraiger, G. and Kühtreiber, N., 1992. Preliminary results of a new Bouguer Map of Austria. *Geodesy and Physics of the Earth: Geodetic Contributions to Geodynamics*. 7th Symposium Nr. 112, 5-10 October, Potsdam. Eds. H. Montag and C. Reigber: Springer Verlag, p. 133.
- Lillie, R.J., Bielik, M., Babuska, V. and Plomerova, J., 1994. Gravity modelling of the lithosphere in the Eastern Alpine - Western Carpathian - Pannonian basin region. *Tectonophysics*, 231, 215-235.
- Lüschen, E., Lammer, B., Gebrande, H., Millahn, K. and Nicolich, R., 2004. Orogenic structure of the Eastern Alps, Europe, from TRANSALP deep seismic reflection profiling. *Tectonophysics*, 388, 85-102.
- Lüschen, E., Borrini, D., Gebrande, H., Lammer, B., Millahn, K., Neubauer, F. and Nicolich, R., 2006. TRANSALP deep crustal Vibroseis and explosive seismic profiling in the Eastern Alps. *Tectonophysics*, 414 (1-4), 9-38.
- Makarenko, I., Legostaeva, O., Bielik, M., Starostenko, V., Dererova, J., Šefara, J., 2002. 3D gravity effects of the sedimentary complexes in the Carpathian-Pannonian region. *Geologica Carpathica*. Vol. 53, special issue, 2002.
- Meurers, B., Ruess, D. and Steinhauser, P., 1987. The Gravitometric Alpine Traverse. In: Flügel H.W. and Faupl P. (eds.), *Geodynamics of the Eastern Alps*. Verlag Deuticke, Wien, 334-344.
- Meurers, B., Steinhauser, P. and Zych, D., 1990. Berechnung der Bougueranomalie im Hochgebirge unter Anwendung eines geologischen Dichtemodells. *Jb. Geol. B.-A.*, 133, 1, 99-109.
- Meurers, B. and Ruess, D., 2007. Compilation of a new Bouguer gravity data base in Austria. *Österreichische Zeitschrift für Vermessung & Geoinformation*, 95. Jahrgang 2007, Heft: 2/2007.
- Meurers, B. and Ruess, D., 2009. A new Bouguer gravity map of Austria. *AJES*, 102, 62-70.
- Nagy, D., 1966. The gravitational Attraction of a right rectangular prism. *Geophysics*, 31, 362-371.
- Oberhauser, R., 1980. *Der Geologische Aufbau Österreichs*, Springer. Wien, New York.
- Sachsenhofer, R. F., Sperl, H. and Wagini, A., 1996. Structure, development and hydrocarbon potential of the Styrian Basin, Pannonian Basin system. In: Wessely, G. & Liebl, W., (eds.): *Oil and Gas in Alpidic Thrustbelts and Basins of Central and Eastern Europe*. - EAGE Spec. Publ., 5, 393-414.
- Schmid, S., Fügenschuh, B., Kissling, E. and Schuster R., 2004. Tectonic map and overall architecture of the Alpine orogen. *Swiss Journal of Geosciences*, 07, 1, 93-117.
- Senftl, E., 1965. *Schwerekarte von Österreich*. Bundesamt für Eich- und Vermessungswesen, Vienna.
- Sobolev, S. and Babeyko, A. Y., 1994. Modeling of mineralogical composition, density and elastic wave velocities in anhydrous magmatic rocks. *Surveys in Geophysics*, 15, 515-544.
- Stampfli, G.M. and Kozur, H.W., 2006. Europe from the Variscan to the Alpine cycles. in *European Lithosphere dynamics*. In: Gee, D.G. & Stephenson, R.A. (eds.), *European Lithosphere Dynamics*, Geological Society London Memoirs, 32, London, pp. 129-145.
- TRANSALP Working Group, 2002. First deep seismic reflection images of the Eastern Alps reveal giant crustal wedges and transcrustal ramps. *Geophys.Res. Lett.*, 29(10), 1452, doi:10.1029/2002GL014911.
- Walach, G., 1987. A digital model of surface rock densities of Austria and the Alpine realm. In: *The gravity field in Austria*. *Geod. Arb. Österr. f. d. Int. Erdmessung*, Neue Folge, Band IV, 3-9, Österr. Komm. f. d. Int. Erdmessung, Graz.

Wortel, M.J.R. and Spakman, W., 2000. Subduction and Slab Detachment in the Mediterranean-Carpathian Region. *Science*, Vol. 290, no. 5498, 1910 - 1917.

Yan, Q.Z. and Mechie, J., 1989. A fine section through the crust and lower lithosphere along the axial region of the Alps. *Geophysical Journal* 98, 465-488.

Ziegler, P.A. und Dèzes, P., 2006. Crustal evolution of Western and Central Europe. *Geological Society, London, Memoirs*; 2006; v. 32; DOI: 1144/GSL.MEM.2006.032.01.03. 43-56.

Received: 5. March 2009

Accepted: 5. November 2009

Oliver SIMEONI & Ewald BRÜCKL[†]

Vienna University of Technology, Institute of Geodesy and Geophysics,
Gusshausstrasse 27-29, A-1040 Vienna, Austria;

[†] Corresponding author, ebrueckl@mail.tuwien.ac.at